Journal of Hazardous Materials 185 (2011) 275–280

Contents lists available at ScienceDirect

Journal of Hazardous Materials

journal homepage: www.elsevier.com/locate/jhazmat

Influence of phosphate on the transport properties of lead in sand

Michael A. Butkus*, Marie C. Johnson

Environmental Engineering Program, Department of Geography and Environmental Engineering, U.S. Military Academy, West Point, NY 10996, United States

ARTICLE INFO

Article history:
Received 3 June 2010
Received in revised form 10 August 2010
Accepted 6 September 2010
Available online 17 September 2010

Keywords:
Lead
Breakthrough curve
Temporal moment analysis
DLVO
Phosphate

ABSTRACT

Temporal moment analysis was used to examine the transport of lead species in sand columns. The influence of sodium phosphate ($PO_{4(aq)}$) and hydroxyapatite (HA) on lead transport was also evaluated. Transport properties of lead microparticles (diameter > 0.45 μm) were a function of electrophoretic mobility: those particles with electrophoretic mobility less than -1×10^{-8} $m^2/V\,s$ exhibited significantly lower dimensionless first temporal moment (θ) and second temporal moment (σ_θ^2). The forms of lead investigated in this work had a tendency to move in sand over a wide pH range. Although the $PO_{4(aq)}$ amendment substantially reduced lead mass recoveries in the sand column effluent, lead microparticles were formed that had a tendency to move rapidly and with minimal dispersion when compared with controls. Treatments with HA provided limited reduction in lead mass recovery and minimal changes in lead transport properties. A colloid stability model was used to predict attachment of lead particles in sand.

Published by Elsevier B.V.

1. Introduction

Lead particles (fines) from bullet fragmentation can make up a large fraction of total lead found on firing ranges [1–3]. Lead particles, produced as lead rounds pierce the soil and undergo weathering processes, yield lead oxides (e.g. PbO) and lead carbonates [1,4,5]. Movement of lead on firing ranges is typically via colloid-facilitated transport [6,7] or transport of lead particles [5]. Sandy soil that is low in clay, iron and aluminum oxides, and organic matter is particularly susceptible to lead movement via colloid transport and leaching [5].

Nriagu [8] proposed the use of phosphate to immobilize aqueous lead ($Pb_{(aq)}$) *in situ* via the formation of low solubility pyromorphites ($Pb_5(PO_4)_3X$, $X = OH^-$, Cl^-, Br^- and F^-). At least 36 treatability studies and 16 mechanistic studies on the use of phosphate to immobilize lead are extant [9]. Hydroxyapatite ($Ca_5(PO_4)_3(OH)$; hereafter referred to as HA) has been used as a source of phosphate for *in situ* lead immobilization but is limited by its dissolution rate [9]. Highly soluble phosphate salts ($PO_{4(aq)}$) can be used to overcome the HA dissolution limitations (although cultural eutrophication concerns are a significant detriment). While some studies have demonstrated that phosphate can retard movement of lead in the environment (cf. [9]), some forms of phosphate treatment have been reported to increase particulate lead concentrations in field water leaching tests [10,11].

The objective of this work is to evaluate the transport properties, via temporal moment analysis, of PbO microparticles and the products formed when PbO microparticles or dissolved ($Pb_{(aq)}$) are combined with $PO_{4(aq)}$ or HA microparticles. A colloid stability model is utilized for predicting the influence of pH on transport behavior of selected lead species in sand.

1.1. Background

In this work, microparticles are defined as having a characteristic length greater than 0.45 μm, and submicron matter is defined as having a characteristic length less than 0.45 μm. Submicron matter includes particles and dissolved substances. Nanoparticles are considered a subset of submicron particles as having a characteristic length of 1–100 nm for at least one dimension and having properties that differ from those of molecules or bulk materials of the same composition [12]. New risk assessment protocols are required for nanoparticles because they may behave differently than conventional chemical compounds [13]. Recently, Liu et al. [14] reported that the dissolution rate differences between galena microparticles and nanoparticles could influence the bioavailability of lead in natural or industrial environments.

Due to the complex nature of reaction, adsorption, and adhesions processes in porous media, transport models based on fundamental parameters are intricate often requiring numerical solution techniques. Consequently other techniques, such as temporal moment analysis, are used for describing relative transport characteristics. Temporal moment analysis can be used to describe one-dimensional transport of matter through intact soil columns via breakthrough curves (BTCs) because BCTs contain all neces-

* Corresponding author. Tel.: +1 845 938 2820; fax: +1 845 938 3339.
E-mail address: Michael.Butkus@usma.edu (M.A. Butkus).

0304-3894/$ – see front matter. Published by Elsevier B.V.
doi:10.1016/j.jhazmat.2010.09.030

sary transport information [15]. Campbell et al. [16] used temporal moment analysis to describe transport of cadmium, copper, and lead in soil columns treated with phosphogypsum, sugar foam, and phosphoric rock.

The mean value of residence time (t_m, s) of a solute or particle moving through a soil column as a function of time (t) is determined from the first temporal moment as follows:

$$t_m = \int_0^\infty t \cdot E(t)\, dt; \tag{1}$$

where $E(t)$ is the probability distribution of the solute travel times (s^{-1}),

$$E_t = \frac{C_{out}(t)}{\sum_0^\infty C_{out}(t) \cdot \Delta t}; \tag{2}$$

where $C_{out}(t)$ = effluent concentration as a function of time (mg/L); Δt = time interval (ca. 5 min).

Dispersion or spreading of the distribution about t_m is described by the second temporal moment (σ^2, s^2) as follows:

$$\sigma^2 = \int_0^\infty (t - t_m)^2 \cdot E(t)\, dt. \tag{3}$$

Normalization of the first and second temporal moments allows for comparison of transport parameters in systems with variations in hydraulic retention time (e.g. when comparing two soil columns with each one having a constant but slightly different volumetric flow rate). Normalization of t_m and σ^2 yield a dimensionless first temporal moment (θ) and second temporal moment (σ_θ^2) in porous media as follows:

$$\theta = \frac{t_m}{(V_{pore}/Q)}; \tag{4}$$

$$\sigma_\theta^2 = \frac{\sigma^2}{(V_{pore}/Q)^2}; \tag{5}$$

where V_{pore} = pore volume (m^3); Q = volumetric flow rate (m^3/s).

Valocchi [17] and Jury and Roth [18] offer comprehensive discussions of temporal moment analysis.

Derjaguin–Landau–Verwey–Overbeek (DLVO) models have been used to describe particle–particle interactions for much of the twentieth century [19,20]. DLVO is predicated on a force (or energy) balance approach, which can be used to predict particle stability in aqueous media. These models account for van der Waals (vdW) and electrostatic forces. van Oss et al. [21] have developed a model ($DLVO_{ex}$), which allows for quantitative determination of DLVO as well as ancillary interfacial forces (Lewis acid/base, AB). The $DLVO_{ex}$ model is often more consistent with experimental findings than DLVO models (cf. [22]). In this work, colloid–sand interactions were modeled using sphere-plate geometry. The model included electrodynamic interactions as described by a retarded vdW model; electrostatic interactions as described by a linear superposition approximation model and Lewis acid/base interactions. This modeling approach is detailed elsewhere [22–25].

2. Materials and methods

Two forms (one dissolved and one particulate) of both lead and phosphate were used in this study. Lead oxide (PbO) powder (99.9% < 10 μm; mean diameter of 2.3 ± 0.87 μm [24]), Aldrich Chemical (Milwaukee, WI), was used to simulate lead microparticles produced from bullet fragmentation. Lead nitrate ($Pb(NO_3)_2$), Fisher Scientific (Fair Lawn, NJ), was used as a source of $Pb_{(aq)}$. Synthetic hydroxyapatite (Bio-Gel HTP), Bio-Rad Laboratories (Rochester, NY) was used as the source of HA microparticles. Dibasic sodium phosphate (Na_2HPO_4), Fisher Scientific (Fair Lawn, NJ), was used as a source of $PO_{4(aq)}$. Samples were prepared in 500 mL of deionized (DI) water as follows: treatment one, 0.800 g $Pb(NO_3)_2$ combined with 0.480 g Na_2HPO_4; treatment two, 0.539 g PbO combined with 0.467 g Na_2HPO_4; treatment three, 0.800 g $Pb(NO_3)_2$ combined with 0.569 g HA; and, treatment four, 0.539 g PbO combined with 0.569 g HA. The PO_4/Pb ratio (1:4) in all four treatments mirrored work by Ma et al. [26]. Stock suspensions were mixed for ca. 20 min, which allowed pH to attain pseudo-steady state values [24] (according to the forms of lead and phosphate), prior to injection in the column. To aid in comparison of the treatments described above, the pH of selected samples was adjusted to 7.2 (pK_{a2} of phosphate) with 1.0 N HNO_3 or 1.0 N NaOH. All glassware was soaked in 10% HNO_3 for a minimum of 24 h and rinsed in DI water to remove adsorbed lead and other contaminants prior to use.

Total lead concentration was quantified using flame atomic absorption spectrophotometry, AA, (GBC 908AA, Arlington Heights, ILL) or inductively coupled plasma optical emission spectrometry, ICP-OES, (Optima 2100DV, PerkinElmer, Shelton, CT). Continued calibration verification (CCV) was conducted with a midrange standard: 10 mg Pb/L for AA or 1.0 mg Pb/L and for ICP-OES. The lead detection limit for AA and ICP-OES were 0.06 mg Pb/L and 0.003 mg Pb/L.

Column experiments were conducted with PVC columns (length 30.5 cm and diameter 2.54 cm) that were wet packed with silica sand (effective size of 1.02 mm and uniformity coefficient < 1.6), US Silica (Berkeley Springs, WV) to obtain a typical porosity of 37% and pore volume of 57 mL/column. Adapters and speed fit valves, United Plastic Corp., (Lima, OH) were used to connect high density polyethylene tubing, United Plastic Corp., (Lima, OH) to both ends of the column. One gram of silica glass wool, Cornins Inc. (Cornings, NY), was placed at the bottom of each column to provide baffling and contain the sand media. Prior to each experiment, the media was washed in up-flow mode (to remove air) with approximately 1500 mL of 1.0 mM NaCl, Fisher Scientific (Fair Lawn, NJ). The column experiments were prepared by withdrawing approximately 10 mL of 1.0 mM NaCl from the top of washed, saturated columns; replacing this aliquot with 5 mL of lead-phosphate stock suspension or 5 mL of a 0.5 M NaCl solution (tracer); refilling with 1.0 mM NaCl; immediately reassembling the column; and, removing remaining air. Columns were then started in down-flow mode under a constant head (typical flow rate of 4.0 ± 1 mL/min and pore water velocity of 2.2 ± 0.5 cm/min) with 1.0 mM NaCl serving as simulated unbuffered ground water. Effluent samples were collected in 125 mL Nalgene HDPE bottles in 20 g increments. Eight mL of this sample was filtered through a 0.45 μm Millipore nylon filter (Bedford, MA) and analyzed for lead. Eighty micro-liters of 16 N HNO_3 was added to the remaining 12 mL of sample (preliminary mass balance experiments demonstrated that all forms of suspended particulate lead used in this work are dissolved using this procedure) and analyzed for (total) lead. Lead concentrations in the stock suspension were determined using the same procedure. A NaCl tracer study was conducted via conductivity measurements. The tracer data were obtained by converting conductivity measurements (μS/L) into concentration (C, mg/L) of NaCl via the following relationship (derived from dilutions of the NaCl stock suspension collected at the same temperature, r^2 = 0.9982):

$$C = 0.5938 \cdot (\text{Conductivity}). \tag{6}$$

Leaching experiments were terminated when approximately 400 mL of sample was collected.

Aging of 500 mL, unmixed, pH 7.2 samples took place under ambient light and temperature conditions in the laboratory. Samples were covered with parafilm prior to aging. Following an aging period of approximately two years (24 ± 2 months), suspensions were remixed, pH was measured, and DI water was added to a final

Table 1
Dimensionless first moment (θ) and second moment (σ_θ^2) transport parameters and mass recovery (%) for: (a) stock suspensions with initial pH 7; (b) following an aging period; and (c) unadjusted pH. The pH of aged samples was adjusted to 7.2 before and after a two-year aging period (standard deviation, Std. Dev.; number of replicates, n).

(a) Transport parameters of stock suspensions at pH 7.2

Sample	θ	Std. Dev.	σ_θ^2	Std. Dev.	Average Mass of lead recovered (μg)	Std. Dev.	n	Notes
PbO submicron	**4.18**	0.34	**2.59**	0.28	**141.2**	15.7	2	
PbO microparticles	**3.65**	0.14	**2.68**	0.36	**81.4**	20.8	2	
$PO_{4(aq)}$ + $Pb_{(aq)}$ microparticles	**1.87**	1.04	**1.85**	2.23	**8.0**	5.6	2	1
$PO_{4(aq)}$ + PbO microparticles	**1.27**	0.79	**0.42**	0.16	**34.8**	22.7	2	1
HA + $Pb_{(aq)}$ submicron	**4.82**		**3.16**		**58.4**	–	2	2
HA + $Pb_{(aq)}$ microparticles	**2.64**	1.78	**2.49**	2.75	**22.4**	25.6	2	
HA + PbO submicron	**3.65**	0.42	**2.38**	0.07	**277.4**	87.4	4	
HA + PbO microparticles	**3.34**	0.40	**2.95**	0.44	**91.5**	40.8	4	

(b) Transport parameters of aged stock suspensions (pH 7.2)

Sample	θ	Std. Dev.	σ_θ^2	Std. Dev.	Average Mass of lead recovered (μg)	Std. Dev.	n	Notes
PbO submicron	**4.81**	–	**2.21**		**16.0**	–	2	2
PbO microparticles	**2.96**	1.82	**2.98**	0.81	**11.9**	14.9	2	
$PO_{4(aq)}$ + Pb(aq) microparticles	**1.70**	0.26	**0.13**	0.13	**15.8**	6.1	2	1
$PO_{4(aq)}$ + PbO submicron	**3.18**	0.55	**0.85**	1.16	**3.2**	1.0	2	
$PO_{4(aq)}$ + PbO microparticles	**2.15**	0.13	**0.43**	0.07	**84.6**	6.7	2	

(c) Transport parameters of stock suspensions with unadjusted pH

Sample	θ	Std. Dev.	σ_θ^2	Std. Dev.	Average mass of lead recovered (μg)	Std. Dev. (μg)	n	pH	Notes
$Pb_{(aq)}$ submicron	**2.56**	0.15	**1.27**	0.18	**1832.1**	90.3	2	3.81	3
NaCl	**3.16**	0.08	**1.50**	0.10	–	–	2	5.35	4
HA + $Pb_{(aq)}$ submicron	**2.73**	0.69	**1.53**	0.04	**665.4**	49.1	4	3.81	
HA + $Pb_{(aq)}$ microparticles	**2.96**	0.74	**2.97**	0.53	**86.4**	70.0	4	3.81	
HA + PbO microparticles	**3.06**	1.37	**2.71**	0.26	**5.4**	9.5	4	9.70	1

[1] Submicron lead was not detected.
[2] Submicron lead for one column was not detected.
[3] Particulate lead was not detected.
[4] Quantified via conductivity.

volume of 500 mL to correct for evaporation. In cases where pH drifted during the aging process, the pH was adjusted back to 7.2 before an aliquot of the suspension was added to the sand columns.

Electrophoretic mobility samples were diluted (500 μL/15mL) with 1 mM $NaNO_3$, Aldrich, (St. Louis, MO), and analyzed with a Brookhaven Instruments Corp. (Holtsville, NY) Zeta PALS particle analyzer.

Sample means were compared using the Student's t test with two sided (two-tail) P values in MS Excel. Sample variances were compared with the F test in MS Excel.

Equilibrium lead species were identified with the MINEQL+ chemical equilibrium modeling system (version 4.5, Environmental Research Software, Hallowell, ME). Model predictions used in this work were based on the molarities of lead and phosphate described above. All model calculations were conducted at 25 °C, with ionic strength corrections, for a system open to the atmosphere.

3. Results and discussion

In an unbuffered sandy firing range soil, sources of lead and phosphate may influence and possibly govern system pH. In this work, reaction products of stock suspensions are evaluated at both unadjusted pH values and pH 7.2 (Table 1). The pH appeared to reach a pseudo-steady state for all samples following the 20-min mixing period, an observation comparable to other studies on lead and phosphate reported in the literature [26,27]. A long term time study (2 years of aging) was included in this work because XRD and modeling data suggested that most suspensions did not reach equilibrium within the 20-min reaction period described above [28]. The pH of aged samples used in the column studies was adjusted back to 7.2, if the pH had drifted, to aid comparison with other results.

The relative tendency of each lead species to move under the influence of ground water was quantified with sand columns. Sand was used because it may represent a worst case condition [25], it is relatively homogeneous, and firing ranges have been located on sandy soils (cf. [29]). With the exception of inlet baffles, the columns were constructed according to the best practices described by Lewis and Sjöstrom [30]. Selected BTCs are presented in Fig. 1 to illustrate trends in effluent data. The ordinate represents a dimensionless concentration, which was obtained by dividing the effluent concentration as a function of time by the concentration injected. The glass wool at the bottom of the column did not have a substantial influence on the fate of lead in this work because digestion experiments and subsequent mass balances on selected sectioned columns, indicated the following: lead was distributed near the top of the column, for treatments where lead was not detected in the effluent; and, lead was distributed throughout the column for treatments where lead was detected in the effluent.

The lead and NaCl tracer data in Fig. 1 are characterized by right hand tails. The slight departure from a perfect Gaussian profile may be due to back mixing in the unbaffled top 10 mL of the column above the media where the tracer and suspensions were added [31]. Because the lengths of the columns were much greater than their radii, the columns were expected to have a sufficient region of uniform flow beyond the inlet zone (in the absence of inlet baffling; cf. [31]). The mass recovery of the NaCl tracer exceeded 100 percent. Because the tracer was estimated via conductivity, which is a nonspecific measure, it is thought that dissolution of impurities may have slightly influenced the mass recovery of the tracer curve. The extent of tailing in the data is similar to laboratory column experiments reported elsewhere (cf. [6,16,32,33]) and is likely due to hydrodynamic processes [32]. The curves representing lead

microparticles were obtained by subtracting concentration of submicron lead (less than 0.45 μm) from concentration of total lead as a function of time. The sequence of declining peaks for microparticles may result from parallel channelling. This type of response is possible because larger mobile particles can be excluded from some pore spaces and travel along central streamlines, which results in shorter paths and faster average travel velocity [34].

Dimensionless first moment and second moment transport parameters and mass recovery data are presented in Table 1(a–c). Insufficient effluent lead precluded transport parameters from being quantified for the following treatments: HA + $Pb_{(aq)}$ (aged); HA + PbO (aged); PbO (unadjusted pH 9.4); $PO_{4(aq)}$ + $Pb_{(aq)}$ (unadjusted pH 5.5); and, $PO_{4(aq)}$ + PbO (unadjusted pH 9.8). Differences in transport properties and mass recovery (*vide infra*) may be the result of several factors including blocking and shadow effects [35], particle size, media (collector) size, media homogeneity, inter-particle forces, hydrodynamic forces (stemming from flow velocity), and, pore plugging (cf. [33]).

Butkus and Johnson [28] reported that electrophoretic mobility was influenced by source of phosphate and lead used in stock suspensions, pH and aging (cf. [28] for a detailed discussion on electrophoretic mobility of these samples). The relationship between electrophoretic mobility and transport parameters, for lead microparticles, is presented in Fig. 2. The lead microparticles with an electrophoretic mobility less than -1×10^{-8} $m^2/V\,s$ traveled with higher average velocity (average θ was significantly lower, $P < 0.0008$). Long range repulsive electrostatic interactions between negatively charged particles and collector surfaces can exclude the particles from negatively charged regions and cause enhanced transport relative to the fluid [36]. Furthermore, dispersion was much less for lead microparticles with electrophoretic mobility less than -1×10^{-8} $m^2/V\,s$ (average σ_θ^2 was significantly lower, $P < 4.57 \times 10^{-5}$). Keller et al. [34] reported that dispersivity can be a function of both the medium and particle size; and that it decreases with increasing particle size. Because the media was not changed and the particles depicted in Fig. 2 were approximately the same size (Butkus and Johnson [28] reported that the mean aggregate diameters of all stock suspension lead microparticles, with unadjusted pH, were between 0.9 μm and 2.8 μm), it is proposed that dissimilarity in σ_θ^2 here derived from variations

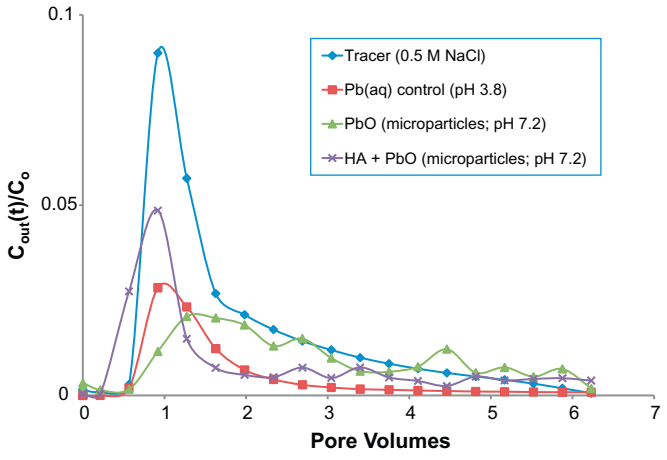

Fig. 1. Breakthrough curves as a function of pore volumes for selected pulse inputs of stock suspensions. The ordinate represents a dimensionless concentration, which was obtained by dividing the effluent concentration as a function of time, $C_{out}(t)$, by the concentration injected, C_o. Curves representing lead microparticles were obtained by subtracting concentration of submicron lead (less than 0.45 μm) from concentration of total lead as a function of time. The $Pb_{(aq)}$ control stock suspension was set to pH 3.8 to minimize formation of particulate lead. The simulated groundwater in all cases was 1.0 mM NaCl.

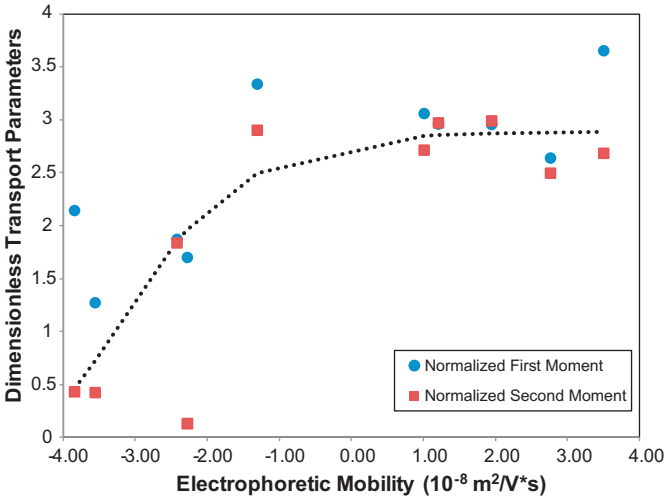

Fig. 2. Relationship between electrophoretic mobility and transport parameters for lead microparticles. The ordinate represents normalized first moment (θ) and second moment (σ_θ^2) transport parameters. A trace has been superimposed on the figure to illustrate trends in the data.

in the long range electrostatic interactions. Because particles with high σ_θ^2 have a tendency to spread in groundwater, electrophoretic mobility can be a useful tool in assessing transport (and subsequent risk) associated with dispersion.

The $Pb_{(aq)}$ control stock ($Pb(NO_3)_2$) was set to a pH of 3.8 to minimize formation of lead microparticles (the objective was to form a solution and lead species > 0.45 μm were not detected). Because the sand media is capable of adsorbing lead complexes [37,38], mass recovery of less than 100% for the $Pb_{(aq)}$ control is not surprising. Unexpectedly, θ derived from the $Pb_{(aq)}$ control was much less than θ of the NaCl tracer ($P < 0.0405$). It is plausible that dissolved complexes of lead were excluded from certain locations or pore spaces via anion exclusion processes [39]. The equilibrium model predicted that Pb^{2+} and $PbNO_3^+$ are predominate aqueous species under these conditions, which implies that anion exclusion may have been minimal in the negatively charged [40] sand media. The model also predicted that $Pb(OH)_{2(s)}$ is formed at equilibrium, which could result in nanoparticles with different transport characteristics than dissolved lead complexes. The relatively low value of θ for the $Pb_{(aq)}$ control supports this hypothesis because formation of lead nanoparticles would be expected to exhibit earlier breakthrough, compared with a NaCl tracer [34,41–43]. In either case, the BCT for lead from the $Pb_{(aq)}$ control, under low pH conditions, is a concern due to considerable lead movement in the sand media.

Adjustment of the PbO stock suspension pH from 9.4 to 7.2 had a substantial influence on the mass recovery of lead (lead was not detected in the column effluent for the pulse of pH 9.4 stock PbO suspension) with slightly more submicron lead than microparticles ($P < 0.083349$). Similarly, Chen et al. [44] reported that lead migration was limited in soils with elevated pH. Butkus and Johnson [28] reported that reduction in pH (from 9.4 to 7.2) resulted in dissolution of PbO and subsequent formation of $Pb(OH)_{2(s)}$ (according to the equilibrium model) or $Pb_3(CO_3)_2(OH)_2$ (according to XRD results for similar samples). Similarly, Fornasiero et al. ([45]; see also [40]) reported that $PbCO_3$ and $Pb_3(CO_3)_2(OH)_2$ appeared to be the predominate species on galena surfaces in suspensions exposed to the atmosphere. Significant differences in θ ($P < 0.0260$) and σ_θ^2 ($P < 0.0313$) between submicron lead derived from the PbO stock suspension at pH 7.2 and the $Pb_{(aq)}$ control suggest that dissimilar species were formed in each case. In addition, submicron lead from the PbO stock suspension at pH 7.2 moved slower (larger θ, $P < 0.0549$) and with more dispersion (larger σ_θ^2, $P < 0.0354$) than the

NaCl tracer. Grolimund et al. [42] also reported that dispersivity of natural and latex colloids was higher than that of a conservative tracer in packed soil columns.

The PbO stock suspension was transformed during the aging process as indicated by a decrease in mass recovery ($P < 0.0619$). Butkus and Johnson [28] reported an increase in percentage of lead greater than 0.45 μm as a result of aging. The shift in particle size could have increased straining [46] and decreased effluent lead mass recoveries. However there was no substantial change in transport parameters as a result of aging. Butkus and Johnson [28] reported that the electrophoretic mobility of PbO starting material decreased as a result of aging, but remained positive; thus, significant changes in θ and σ_θ^2 would not be expected according to Fig. 2.

Stock suspensions created via addition of $PO_{4(aq)}$ to both forms of lead resulted in low mass recovery. However, the fraction of lead microparticles formed in the $PO_{4(aq)}$ treatment stock suspensions that passed through the column had a tendency to move rapidly, with minimal dispersion when compared with the $Pb_{(aq)}$ and PbO effluent data. For example, θ of microparticles from the PbO, pH 7.2, stock suspension was 3.65 while θ of microparticles from the PbO + $PO_{4(aq)}$ treatment was 1.27 ($P < 0.0530$). Similarly, σ_θ^2 of microparticles from the PbO, pH 7.2, stock suspension was 2.68 while σ_θ^2 from the PbO + $PO_{4(aq)}$ treatment was 0.42 ($P < 0.0145$). Colloid-facilitated transport of pollutants, such as lead, is a significant problem as colloids can travel over long distances with movement often being limited only by the instability of the porous medium and clogging [47]. The enhanced velocity of the lead products formed via the $PO_{4(aq)}$ treatment may be a detriment. Mass recovery and transport parameters of effluent lead from the $PO_{4(aq)}$ + $Pb_{(aq)}$ treatment stock suspension did not change significantly with aging, which suggests that the method proposed by Nriagu [8] on the use of $PO_{4(aq)}$ to retard movement of lead is efficacious (relative to mass recovery) under selected conditions. Aging of the $PO_{4(aq)}$ + PbO stock suspension resulted in a slight increase in effluent lead microparticles ($P < 0.0970$) above the $PO_{4(aq)}$ + PbO stock suspension and significant increase relative to the aged PbO, pH 7.2 stock suspension ($P < 0.0244$).

Table 2
Surface thermodynamic properties and parameters of particles and media used in the $DLVO_{ex}$ colloid stability model.

Surface	Zeta potential (mV)	Ref.
PbO (pH 9.4)	44.4	This work
PbO (pH 7.2)	49.2	This work
$Pb_3(CO_3)_2(OH)_2$[a]	−20	[40][b]
Sand (SiO_2) in the absence of dissolved lead (pH 9.4)	−28.7	This work
Sand in the presence of dissolved lead (pH 7.2)	8.0	[40][b]
Sand in the presence of lead carbonate	−28.7	This work
Lifshitz–van der Waals (LW) surface free energy (mJ/cm²)		
PbO	32.2	[48]
$Pb_3(CO_3)_2(OH)_2$	38.9	[48]
Sand (SiO_2)	39.2	[49]
Lewis acid base (AB) surface free energy (mJ/cm²)		
PbO	22.7	[48]
$Pb_3(CO_3)_2(OH)_2$	5.46	[48]
Sand (SiO_2)	11.5	[49]
Diameter (μm)		
PbO (pH 9.4)	2.32	[28]
PbO (pH 7.2)[c]	0.45	This work
$Pb_3(CO_3)_2(OH)_2$[c]	0.45	This work

[a] According to Rashchi et al. [40], the zeta potential of $Pb_3(CO_3)_2(OH)_2$ is similar to $PbCO_3$ above pH 4.

[b] The zeta potential in Ref. [40] was quantified in a 1 mM KNO_3 background electrolyte.

[c] A diameter of 0.45 μm was assumed based on the distribution of lead presented in Table 1.

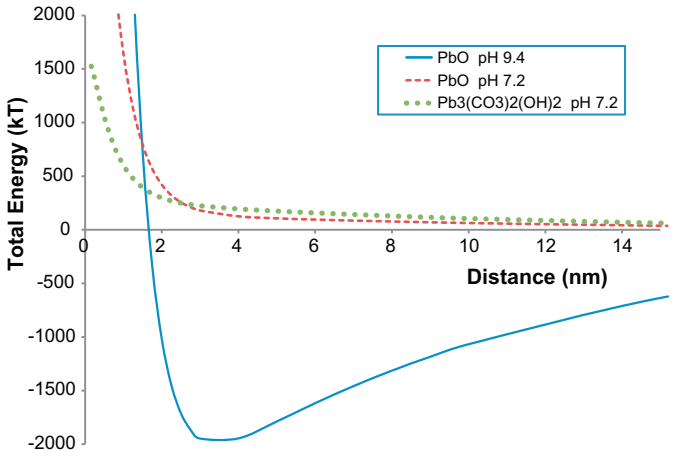

Fig. 3. Energy (kT) predictions from a $DLVO_{ex}$ colloid stability model between a sand (modeled as SiO_2) collector and lead particles. Values used to develop the model are presented in Table 2.

Mass recoveries from the HA treatment of PbO, pH 7.2, stock suspension were greater than mass recoveries from the PbO, pH 7.2, stock suspension. However, the normalized transport parameters were approximately the same for submicron (θ, $P < 0.2012$ and σ_θ^2, $P < 0.2291$) and microparticle (θ, $P < 0.3690$ and σ_θ^2, $P < 0.5000$) fractions of effluent lead. The mechanism of increased effluent lead, for the HA + PbO pH 7.2 treatment, remains unknown. Although mass recovery of submicron lead for the HA + $Pb_{(aq)}$, pH 3.81, stock suspension was significantly less than submicron effluent lead from $Pb_{(aq)}$ control ($P < 2.07197E{-}05$), transport properties were not significantly different (θ, $P < 0.7665$ and σ_θ^2, $P < 0.3047$) compared with the $Pb_{(aq)}$ control. However, the lead microparticles in the column effluent, formed via HA + $Pb_{(aq)}$ treatment (pH 3.8) had larger σ_θ^2 than the $Pb_{(aq)}$ control ($P < 0.0143$), which implies that the mobile fraction of particulate lead in this treatment might have a greater tendency to spread by dispersion in the subsurface than the control.

A $DLVO_{ex}$ colloid stability model was used to predict attachment of lead to sand under the pH conditions in this work. Surface free energy components and selected zeta potential measurements were taken from the literature (Table 2). Rashchi et al. [40] reported that the zeta potential of silica ($7 < pH < 12$) was positive in the presence of Pb^{2+} and negative in the presence of lead carbonate. These variations in the sand (collector) zeta potential were incorporated into the model. Predictions from the $DLVO_{ex}$ model are presented in Fig. 3. The model predicted that PbO microparticles adhere to sand (modeled as SiO_2) in a deep secondary minimum at pH 9.4, which is consistent with experimental findings (lead was not detected in the column effluent). The model predicted that particle attachment in the primary or secondary minima is not expected for PbO and $Pb_3(CO_3)_2(OH)_2$ at pH 7.2. These model predictions are consistent with trends in effluent lead data for the PbO stock suspension, at pH 7.2, presented in Table 1. A classic DLVO model (data not shown) was unable to predict effectively lead particle–sand interactions in these systems. The agreement of $DLVO_{ex}$ model results with experimental results suggests the importance of Lewis acid–base interactions in this system.

4. Conclusion

Transport properties (normalized first and second temporal moments) varied as a function of lead species and correlated well with electrophoretic mobility. The $DLVO_{ex}$ model predicted attachment of particulate lead to the sand media. These constructs could be integrated into existing lead transport models to enhance their prediction capabilities.

Most forms of lead investigated in this work had a tendency to move in sand over a wide pH range, which demonstrates the need for lead remediation on firing ranges. Based on the conditions set in this work, $PO_{4(aq)}$ significantly retarded the mobility of $Pb_{(aq)}$ and PbO, although some lead-phosphate species in these treatments moved with a higher pore water velocity than the lead controls. The HA amendment had a limited influence on lead transport properties and it increased lead mass recoveries in some cases. It is suggested that new forms of phosphate amendments be developed to overcome the limitations identified in this study.

Acknowledgments

The technical assistance of Mr. Anand Shetty, Major Phil Dacunto, Colonel Jason Lynch and Major James Jordano, Department of Geography and Environmental Engineering, United States Military Academy is greatly appreciated. This project was supported by grants from the US Army Corps of Engineers Engineer Research Development Center (ERDC). Although the research presented in this paper has been undertaken by personnel employed by US Military Academy, it does not necessarily reflect the views of the Academy or the US Army.

References

[1] D.W. Hardison, L.Q. Ma, T. Luongo, W.G. Harris, Lead contamination in shooting range soils from abrasion of lead bullets and subsequent weathering, Sci. Total Environ. 328 (2004) 175–183.
[2] J. Clausen, N. Korte, The distribution of metal sin soils and pore water at three U.S. military training facilities, Soil Sediment Contam. 18 (2009) 546–563.
[3] J. Lewis, J. Sjöstrom, U. Skyllberg, L. Hägglund, Distribution, chemical speciation, and mobility of lead and antimony originating from small arms ammunition in a course-grained unsaturated surface sand, J. Environ. Qual. 39 (2010) 863–870.
[4] S.S. Jørgensen, M. Willems, The fast of lead in soils: the transformation of lead pellets in shooting-range soils, Ambio 16 (1987) 11–15.
[5] X. Cao, L.Q. Ma, M. Chen, D.W. Hardison Jr., W.G. Harris, Weathering of lead bullets and their environmental effects at outdoor shooting ranges, J. Environ. Qual. 32 (2003) 526–534.
[6] S. Hu, X. Chen, J. Shi, Y. Chen, Q. Lin, Particle-facilitated lead and arsenic transport in abandoned mine sites soil influenced by simulated acid rain, Chemosphere 71 (2008) 2091–2097.
[7] X. Yin, B. Gao, L.Q. Ma, U.K. Saha, H. Sun, G. Wang, Colloid-facilitated Pb transport in two shooting-range soils in Florida, J. Hazard. Mater. 177 (2010) 620–625.
[8] J.O. Nriagu, Lead orthophosphates—IV. Formation and stability in the environment, Geochim. Cosmochim. Acta 38 (1974) 887–898.
[9] M. Chrysochoou, D. Dermatas, D.G. Grubb, Phosphate application to firing range soils for Pb immobilization: the unclear role of phosphate, J. Hazard. Mater. 144 (2007) 1–14.
[10] R. Stanforth, C.F. Yap, R. Nayar, Effects of weathering on treatment of lead contaminated soils, J. Environ. Eng. 131 (2005) 38–48.
[11] D.W. Kilgour, R.B. Moseley, M.O. Barnett, K.S. Savage, P.M. Jardine, Potential negative consequences of adding phosphorous-based fertilizers to immobilize lead in soil, J. Environ. Qual. 37 (2008) 1733–1740.
[12] S.F. Hansen, B.H. Larsen, S.I. Olsen, A. Baun, Categorization framework to aid hazard identification of nanomaterials, Nanotoxicology 1 (3) (2007) 243–250.
[13] M.R. Wiesner, V.L. Gregory, K. Jones, M.F. Hochella, R.T. Di Giulio, E. Casman, E. Bernhardt, Decreasing uncertainties in assessing environmental exposure, risk and ecological implications of nanomaterials, Environ. Sci. Technol. 43 (2009) 6458–6462.
[14] J. Liu, D.M. Aruguete, M. Murayama, M.F. Hochella Jr., Influence of size and aggregation on the reactivity of an environmentally and relevant nanomaterial (PbS), Environ. Sci. Technol. 43 (2009) 8178–8183.
[15] G. Sposito, W.A. Jury, The lifetime probability density function for solute movement in the subsurface zone, J. Hydrol. 102 (1988) 503–518.
[16] C.G. Campbell, F. Garrido, V. Illera, M.T. Garcia-Gonzalez, Transport of Cd, Cu and Pb in an acid soil amended with phosphogypsum, sugar foam and phosphoric rock, Appl. Geochem. 21 (2006) 1030–1043.
[17] A.J. Valocchi, Use of temporal moment analysis to study reactive solute transport in aggregated porous media, Geoderma 46 (1990) 233–247.
[18] W.A. Jury, K. Roth, Transfer Functions and Solute Movement Through Soil, Birkhauser Verlag, Basel, Switzerland, 1990.
[19] B.V. Derjaguin, L.D. Landau, Theory of the stability of strongly charged lyophobic sols and of the adhesion of strongly charged particles in solutions of electrolytes, Acta Physicochim. U.S.S.R. 14 (1941) 633.
[20] E.J.W. Verwey, J.Th.G. Overbeek, Theory of the Stability of Lyophobic Colloids, Elsevier, Amsterdam, 1948.
[21] C.J. van Oss, M.K. Chaudhury, R.J. Good, Interfacial Lifshitz–van der Waals and polar interactions in macroscopic systems, Chem. Rev. 88 (1988) 927.
[22] D. Grasso, K. Subramaniam, M.A. Butkus, K. Strevett, J. Bergendahl, A review of non-DLVO interactions in environmental colloidal systems, Rev. Environ. Sci. Biotechnol. 1 (2002) 17–38.
[23] J. Gregory, Interaction of unequal double layers at constant charge, J. Colloid Interface Sci. 51 (1975) 44.
[24] J. Gregory, Approximate expressions for retarded van der Waals interaction, J. Colloid Interface Sci. 83 (1981) 138.
[25] C.J. van Oss, Interfacial Forces in Aqueous Media, Marcel Dekker, NY, 1994.
[26] L.Q. Ma, S.J. Traina, T.J. Logan, J.A. Ryan, In situ lead immobilization by apatite, Environ. Sci. Technol. 27 (1993) 1803–1810.
[27] S. Raicevic, T. Kaludjerovic-Radoicic, A.I. Zouboulis, In situ stabilization of toxic metals in polluted soils using phosphates: theoretical prediction and experimental verification, J. Hazard. Mater. B117 (2005) 41–53.
[28] M.A. Butkus, M.C. Johnson, Reevaluation of phosphate as a means of retarding lead transport from sandy firing ranges, Soil Sediment Contam., in press.
[29] J. Clausen, J. Robb, D. Curry, N. Korte, A case study of contaminants on military ranges: Camp Edwards Massachusetts, USA, Environ. Poll. 129 (2004) 13–21.
[30] J. Lewis, J. Sjöstrom, Optimizing the experimental design of soil columns in saturated and unsaturated transport experiments, J. Contam. Hydrol., doi:10.1016/j.jconhyd.2010.04.001.
[31] D.A. Barry, Effect of nonuniform boundary conditions on steady flow in saturated homogenous cylindrical soil columns, Adv. Water Resour. 32 (2009) 522–531.
[32] N. Huber, T. Baumann, R. Niessner, Assessment of colloid filtration in natural porous media by filtration theory, Environ. Sci. Technol. 34 (2000) 3774–3779.
[33] T.K. Sen, K.C. Khilar, Review on subsurface colloids and colloid-associated contaminant transport in saturated porous media, Adv. Colloid Interface Sci. 119 (2006) 71–96.
[34] A.A. Keller, S. Sirivithayapakorn, C.V. Chrysikopoulos, Early breakthough of colloids and bacteriophage MS2 in a water-saturated sand column, Water Resour. Res. 40 (2004), W08304, 11 PP.
[35] C.H. Ko, M. Elimelech, The "shadow effect" in colloid transport and deposition dynamics in granular porous media: measurements and mechanisms, Environ. Sci. Technol. 34 (2000) 3681–3689.
[36] J.C. Šimůnek, C. He, L. Pang, S.A. Bradford, Colloid-facilitated solute transport in variably saturated porous media: numerical model and experimental verification, Vadose Zone J. 5 (2006) 1035–1047.
[37] A. Manceau, M.C. Boisset, G. Sarret, J.L. Hazemann, M. Mench, P. Cambier, R. Prost, Direct determination of lead speciation in contaminated soils by EXAFS spectroscopy, Environ. Sci. Technol. 30 (1996) 1540–1552.
[38] E.J. Elzinga, D.L. Sparks, X-ray absorption spectroscopy study of the effects of pH and ionic strength of Pb(II) sorption to amorphous silica, Environ. Sci. Technol. 36 (2002) 4352–4357.
[39] H. Gvirtzman, S.M. Gorelick, Dispersion and advection in unsaturated porous media enhanced by anion exclusion, Nature 352 (1991) 793–795.
[40] F. Rashchi, Z. Xu, J.A. Finch, Adsorption on silica in Pb– and Ca–SO_4–CO_3 systems, Coll. Surf. A 132 (1998) 159–171.
[41] H. Small, Hydrodynamic chromatography: a technique for size analysis of colloidal particles, J. Colloid Interface Sci. 48 (1974) 147–161.
[42] D. Grolimund, M. Elimelech, M. Borkovec, K. Barmettler, R. Kretzschmar, H. Sticher, Transport of in situ mobilized colloidal particles in packed soil columns, Environ. Sci. Technol. 32 (1998) 3562–3569.
[43] N. Massei, M. Lacroix, H.Q. Wang, J.P. Dupont, Transport of particulate material and dissolved tracer in a highly permeable porous medium: comparison of the transfer parameters, J. Contam. Hydrol. 57 (2002) 21–39.
[44] M. Chen, S.H. Daroub, L.Q. Ma, W.G. Harris, X. Cao, Characterization of lead in soils of a rifle/pistol shooting range in central Florida, USA, Soil Sediment Contam. 11 (2002) 1–17.
[45] D. Fornasiero, F. Li, J. Ralston, Oxidation of galena: II. Electrokinetic study, J. Colloid Interface Sci. 164 (2) (1994) 345–354.
[46] S.A. Bradford, S. Torkzaban, S.L. Walker, Coupling of physical and chemical mechanisms of colloid straining in saturated porous media, Water Res. 41 (2007) 3012–3024.
[47] D. Grolimund, M. Borkovec, Colloid Facilitated transport of strongly sorbing contaminants in natural porous media: mathematical modeling and laboratory column experiments, Environ. Sci. Technol. 39 (2005) 6378–6386.
[48] B. Jańczuk, E. Chibowski, W. Wójcik, M.C. Guindo, F. González-Caballero, Surface free energy of some lead compounds compared to galena, Mater. Chem. Phys. 37 (1994) 64–67.
[49] C.J. van Oss, R.F. Giese, W. Wu, Surface and electrokinetic properties of clays and other mineral particles, untreated and treated with organic or inorganic cations, J. Dispers. Sci. Technol. 17 (1996) 527.